Enhanced Intraoperative Visualization for Brain Surgery:
A Prototypic Simulated Scenario

Z. Salah[1,2], B. Preim[1], A. Samii[3], R. Fahlbusch[3], and G. Rose[2]

[1] *University of Magdeburg, Institute for Simulation and Graphics, Magdeburg, Germany*
[2] *University of Magdeburg, Institute for Electronics, Signal Processing and Communications, Magdeburg, Germany*
[3] *International Neuroscience Institute, Hannover, Germany*

Contact: Zein.Salah@ovgu.de

Abstract:

Due to the required high precision and reliability, image guidance is increasingly being adapted in neurosurgery, where correspondences between the patient and scanned data are viewed on multiple displays. In this paper, we present a prototype for an augmented reality system that provides enhanced intraoperative visualization within the optical surgery microscope image. For this purpose, relevant targeted and risk structures are extracted from registered patient data and overlaid on the real scene. Similarly, supportive information of underlying anatomy can be superimposed, which includes, amongst others, shape and depth information of tumors, and interactively selected tomographical slices. The overall advantage is a more ergonomic hand-eye coordination, a more accurate delineation of targeted structures and better protection of risk anatomy.

Keywords: Medical Augmented Reality, Intraoperative Visualization, Medical Navigation

1 Problem

Medical navigation systems help physicians to establish correspondences between locations in an acquired patient dataset and the patient's physical body during navigated surgeries. This is highly advantageous in neurosurgery, where high precision is demanded. In a microscope-assisted surgery, however, this requires the surgeon to switch between the microscope and wall-mounted or computer displays. By incorporating augmented reality, it becomes possible to view patient data directly in the 3D context of the patient himself. This may provide an in-place insight into the patient body, which, for example, would help defining the entry point and the trajectory of a biopsy needle [7]. Some systems have been introduced that provide enhanced endoscopic views that are paired with synthesized virtual renderings generated from the same view [4, 6]. Other systems tried to modify the design of operating binoculars [2] and microscopes [3] to allow for data augmentation.

In this paper, we present a prototype for enhancing intraoperative visualization within the operating microscope, by augmenting the video stream with relevant patient data from different diagnostic and intraoperative imaging modalities. The advantage is a better localization of targeted lesions (e.g. tumor) and the protection of hidden risk structures like blood vessels and neural connections. The prototype includes the different components of a navigated procedure: tracking, calibration, registration, and rendering, which are described in the following section.

2 Methods

For our prototype, we implement a marker-based optical tracking system and use a tablet PC with a high resolution built-in camera to simulate the surgical microscope. A phantom model of the head simulates the patient. In the context of this paper, we refer to the tablet PC camera as the *video camera* and to the camera of the tracking system as the *tracker camera*. At a first step, the system cameras are calibrated to compute their intrinsic geometrical parameters. This is performed by capturing several photos of a special checkerboard pattern, with the tracker camera, from different

locations and orientations. Afterwards, MATLAB's Camera Calibration Toolbox[1] is used to calculate the focal length, principal point, and skew and distortion coefficients of the camera. The same process is performed for the video camera. The intrinsic calibration procedure is performed only once and the camera parameters are stored.

A tracking server continuously captures a video stream with the tracker camera (Logitech QuickCam Pro 9000; Resolution: 1280×720 pixel; 30 fps). At each frame, the system searches for predefined markers and, for each detected marker, computes the 3D position and orientation in the camera coordinate system. Pose information of all detected markers are broadcasted to the tablet PC (and other devices, if necessary) over a WLAN connection.
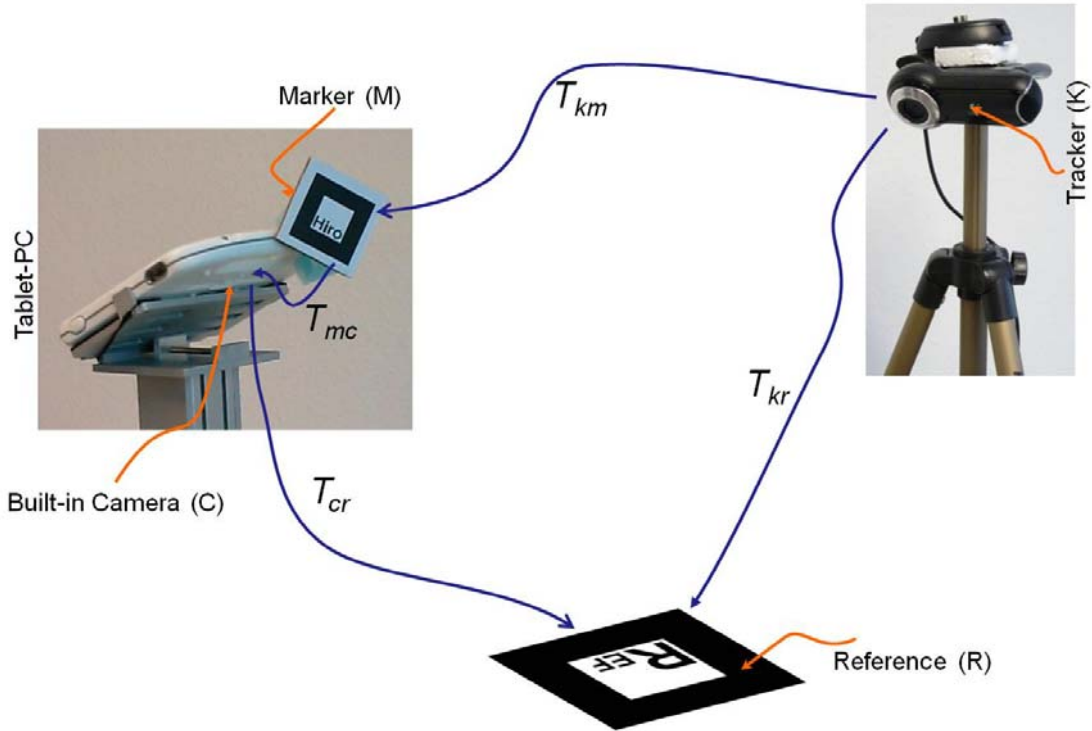

Figure 1: Calibration of the video camera with the tracker.

In a second step, the video camera (C) is calibrated with respect to the tracking system (K). This is achieved, as shown in Figure 1, using a common reference marker (R) that is visible (only at the calibration step) to both cameras. A second marker (M) is fixed to the tablet PC to allow for tracking it during the operation. The arrows show the transformations between the different coordinate systems. For example, T_{kr} is the transformation from the reference R to the tracker K. Following this chain of transformations, the transformation from the marker M to the video camera C can be calculated as follows:

$$T_{mc} = T_{cr}.T_{kr}^{-1}.T_{km} \qquad (1)$$

This one-step calibration is performed fully automatically. The resulting transformation remains valid as long as the marker M does not move relative to the video camera. At operation time, the patient is fixed with respect to the reference marker, which, in turn, will no more be visible to the video camera C. Fortunately, the transformation T_{cr} can now be computed using:

$$T_{cr} = T_{mc}.T_{km}^{-1}.T_{kr} \qquad (2)$$

Since T_{mc} is constant from the previous step and T_{kr} is inherently fixed, T_{cr} is only dependent on T_{km}, i.e. on the tracking data of the marker M.

---

[1] http://www.vision.caltech.edu/bouguetj/calib_doc/

To create correct correspondences between the patient (phantom model) and the scanned dataset, we adapt a paired-point rigid registration scheme. In essence, we choose a set of points in the patient coordinate system whose positions can be precisely defined by the tracking system. A second set of corresponding points is interactively selected from the scanned dataset (in our case, four points are selected from a scanned CT image). Absolute positions of these points are calculated considering their voxel coordinates and image spacing. The two sets of points are finally registered utilizing a least square fitting approach. Particularly, the rigid registration transformation T_{reg} is composed as:

$$\boldsymbol{T_{reg}} = R*T \qquad\qquad (3)$$

Here, T is a translation calculated through the shift of centroids of the two input point sets, and R is calculated using singular value decomposition, as described in [1].

At rendering time, the frame captured by the video camera is first rendered as a background. Additional (virtual) objects are then rendered/overlaid using OpenGL, where the MODELVIEW Matrix is computed as $T_{cr}.T_{reg}$. Examples of objects that can be overlaid are 3D reconstructions of segmented structures like blood vessels and tomographical slices from the anatomy dataset. For certain structures, e.g. tumors, an enhanced visualization of shape and depth information can also be provided. This is achieved by extracting the planar contours of the tumor at successive depths perpendicularly to the viewing direction, as shown in Figure 2b. For this purpose, we calculate the intersection of the tumor surface model with a cutting plane, while changing the depth of the plane. Depth information is conveyed via depth cueing, i.e. the transparency of a contour is defined as a linear function of its depth so that deeper contours appear more transparent. This contour visualization assists the surgeon to better determine the shape and extent of the tumor at different depth levels.

To visualize tomographical slices, we adapt an optimized cross sectioning algorithm [5] to compute the slices at the desired position and orientation. This algorithm applies an incremental approach to compute, for each pixel location in the cross section plane, the corresponding 3D location in the volumetric data, and evaluates the final pixel intensity using tri-linear interpolation. The generated slice image is then used as texture for a rectangle, which is in turn rendered in the real scene with the correct pose. Thereby, the spatial resolution (dimension and spacing) of the dataset and the cross section are considered in order to exactly reflect the spatial proportion with the patient and environment, whose coordinate system is represented in millimeter.
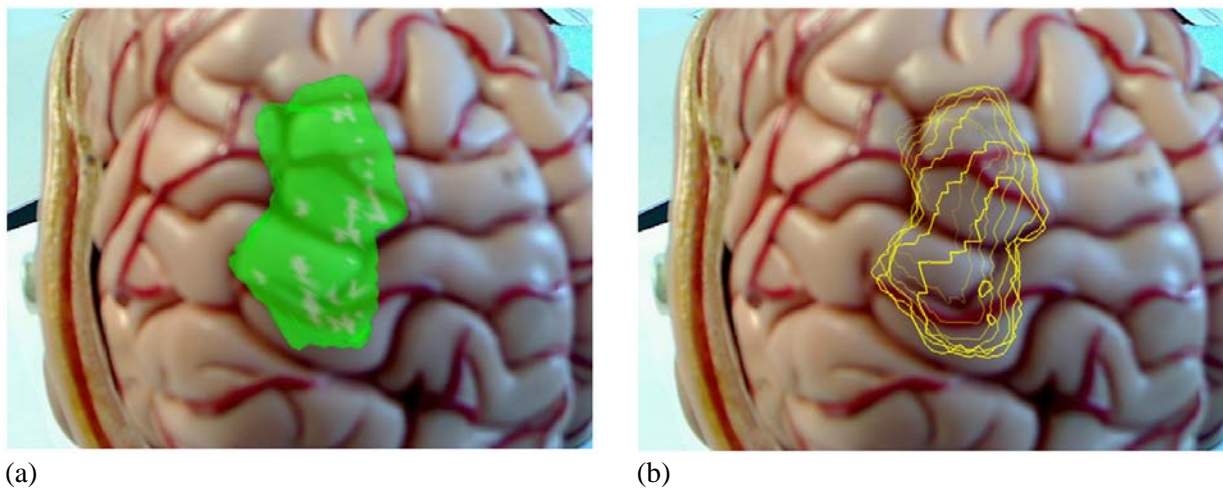

(a) (b)

Figure 2: Augmented views from the presented system: (a) A tumor is blended over the optical image; (b) Contours of the tumor at successive depth levels (distance=2mm), deeper contours are more transparent.
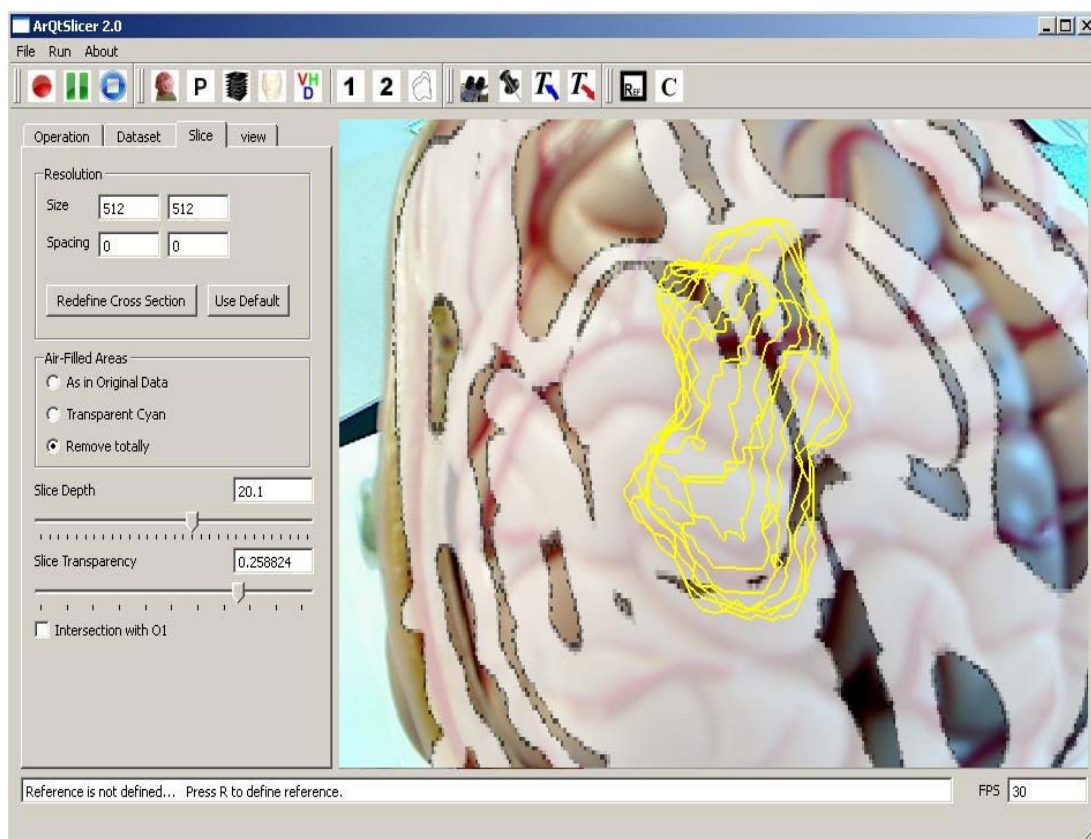
Figure 3: GUI of the visualization module: The widget shows a tomographical slice that is computed perpendicular to the viewing vector and superimposed on the operation field, together with an augmented display of the tumor contours.

3   Implementation and Results

The software components of our system have been implemented with C++ (Microsoft Visual Studio 2005). Rendering was performed using OpenGL. The GUI, shown in Figure 3, was implemented using the Qt[2] library. For our current implementation of the prototype, we relied on marker-based tracking provided by the ARToolkit[3], which allows for multiple-marker tracking in real time. However, due to the inaccurate calibration provided by ARToolkit, we decided to recalibrate camera parameters using MATLAB, as stated in the previous section. Consequently, the MATLAB based calibration was much more accurate regarding 3D overlay and depth estimation processes.

To simulate an operation scenario, a phantom model of the head is CT-scanned and an imaginary tumor is manually embedded in the CT dataset. The tumor is segmented from the dataset, partially based on Kitware's Insight Segmentation and Registration Toolkit ITK[4], and a 3D model is reconstructed using the Marching Cubes algorithm. Afterwards, the video camera is calibrated with respect to the tracker (extrinsic calibration). After this one-step calibration, the reference marker R must stay fixed with respect to the tracker camera. Also, the tracking marker M must stay fixed with respect to the video camera. The phantom model is then registered to the scanned data, using a small set of correspondence point pairs, including the corners of the reference R. Finally, augmentation into the video stream can start.

Figure 2 shows some snapshots of our prototype for enhanced visualization in a brain tumor surgery scenario. In Figure 2a, an augmented view of a malignant tumor (green) is presented. In Figure 2b, boundaries of the tumor at successive depth planes (distance=2mm) are displayed, where transparency is defined as a function of depth. Figure 3 depicts the

---

[2] http://qt.nokia.com/
[3] http://www.hitl.washington.edu/artoolkit/
[4] http://www.itk.org/

GUI of the whole visualization module, showing an augmented view of the tumor contours (yellow) and an interactively selected tomographical slice from the CT dataset, blended over the optical image. In this context, the cross sectioning algorithm allows for a computation and rendering rate of about 30 fps.

4 Discussion

We introduced a prototype for enhancing intraoperative visualization within the operating microscope, by augmenting the video stream with relevant operational information. This prototype is a PC / tablet PC based simulation of the aimed scenario using a surgery microscope. The essential components of the system (tracking, calibration, registration, and rendering) have been described. The objects of interest are extracted from registered pre- and intraoperative patient data. This results in a better localization of targeted lesions and the protection of proximate risk structures, like blood vessels or certain functional units. From surgical point of view, the system offers a good usability and added value to the procedure. Our next step is the transfer of the approach into a real surgery suite. Thereby, the surgical microscope will replace our tablet PC based optical/visualization device, and the camera tracking will be performed by an infrared tracking system. Although the system initially was aimed for neurosurgery applications like brain tumor and hypophysis surgeries, the concept can be transferred to several other surgery procedures.

Acknowledgment

5 References

[1] K. Arun, T. Huang, and S. Blostein, Least-Squares Fitting of Two 3D Point Sets, IEEE Transactions on Pattern Analysis and Machine Intelligence, 9(5):698–700, 1987.

[2] W. Birkfellner, M. Figl, K. Huber, F. Watzinger, F. Wanschitz, J. Hummel, R. Hanel, W. Greimel, P. Homolka, R. Ewers, and H. Bergmann. A Head-Mounted Operating Binocular for Augmented Reality Visualization in Medicine-Design and Initial Evaluation. IEEE Transactions on Medical Imaging, 21(8):991–997, 2002.

[3] P. Edwards, A. King, C. Maurer, D. de Cunha, D. Hawkes D. Hill, R. Gaston, M. Fenlon, S. Chandra, A. Strong, C. Chandler, am M. Gleeson, Design and Evaluation of a System for Microscope-Assisted Guided Interventions (MAGI). IEEE Transactions on Medical Imaging, 19(11):1082–1093, 2000.

[4] R. Lapeer, M. Chen, G. Gonzalez, A. Linney, and G. Alusi. Image-Enhanced Surgical Navigation for Endoscopic Sinus Surgery: Evaluating Calibration, Registration and Tracking. The International Journal of Medical Robotics and Computer Assisted Surgery, 4(1):32–45, 2008.

[5] Z. Salah, B. Preim, and G. Rose. An Approach for Enhanced Slice Visualization utilizing Augmented Reality: Algorithms and Applications, Proc. of PICCIT, 2010.

[6] R. Shahidi, M. Bax, C. Maurer, J. Johnson, E. Wilkinson, B. Wang, J. West, M. Citardi, K. Manwaring, and R. Khadem. Implementation, Calibration and Accuracy Testing of an Image-Enhanced Endoscopy System. IEEE Transactions on Medical Imaging, 21(12):1524–1535, 2002.

[7] F. Wacker, S. Vogt, A. Khamene, J. Jesberger, S. Nour, D. Elgort, F. Sauer, J. Duerk, and J. Lewin. An Augmented Reality System for MR Image-guided Needle Biopsy: Initial Results in a Swine Model. Radiology, 238(2):497–504, 2006.